J. Earth Syst. Sci. (2023)132 111
https://doi.org/10.1007/s12040-023-02121-1

On rogue La Niñas, with below-average monsoon rainfall

Sulochana Gadgil[1,*], Mark A Cane[2] and P A Francis[3,4]

[1]*Centre for Atmospheric and Oceanic Sciences, Indian Institute of Science, Bangalore 560 012, India.*
[2]*Lamont Doherty Earth Observatory, Columbia University, Palisades, New York 10964, USA.*
[3]*Centre for Excellence in Marine Studies, University of Mumbai, Mumbai 400 098, India.*
[4]*Indian National Centre for Ocean Information Services, Ministry of Earth Sciences, Govt. of India, Hyderabad 500 090, India.*
**Corresponding author. e-mail: sulugadgil@gmail.com*

MS received 12 January 2023; revised 11 April 2023; accepted 11 April 2023

Prediction of the seasonal monsoon rainfall over India relies largely on the well-known relationship with El Niño and Southern Oscillation (ENSO) and is possible because reasonably reliable seasonal predictions of ENSO are now available. Usually, the cold phase of ENSO is associated with above-normal monsoon rainfall and the warm phase of ENSO with below-normal rainfall. There are, however, exceptions: years in the cold phase of ENSO with below-normal monsoon rainfall and even drought conditions. We term these exceptional events 'rogue La Niñas'. Clearly, an explanation of these exceptional cases will improve the predictive skill. Here we show that for the part of the Arabian Sea, east of the upwelling region and north of the equatorial belt (60°–70°E, 10°–23°N), the correlation of outgoing longwave radiation with Indian summer monsoon rainfall is even higher than that with the equatorial central Pacific associated with ENSO. Convection over this region is triggered by ENSO, but is modulated by the underlying sea surface temperature (SST). There is a minimum of SST of about 28.1°C above which the convection over the Arabian Sea is high enough and there are no rogue La Niñas. Furthermore, we show that, in this region, the SST of June–September is related to the SST of April–May. When April–May SST is >29.6°C, June–September mean SST is always >28.1°C and there are no rogue La Niñas; the monsoon rainfall is always normal or above normal as expected with a La Niña. Thus the chance of a rogue La Niña can be predicted from the April–May SST of the Arabian Sea.

Keywords. Indian summer monsoon; El Niño and Southern Oscillation; La Niña; Arabian Sea.

1. Introduction

Since a large fraction of the rainfall over the Indian region occurs during June–September, as in most studies, we focus on the monsoon rainfall during this summer monsoon season. The convective region with deep clouds associated with the Indian summer monsoon rainfall (figure 1a) is a part of the larger scale low outgoing longwave radiation (OLR) region extending over part of the Arabian Sea, equatorial Indian Ocean, Bay of Bengal and the West Pacific (figure 1b). The large-scale summer monsoon rainfall over the Indian region is sustained by cloud bands propagating northward

Published online: 07 July 2023

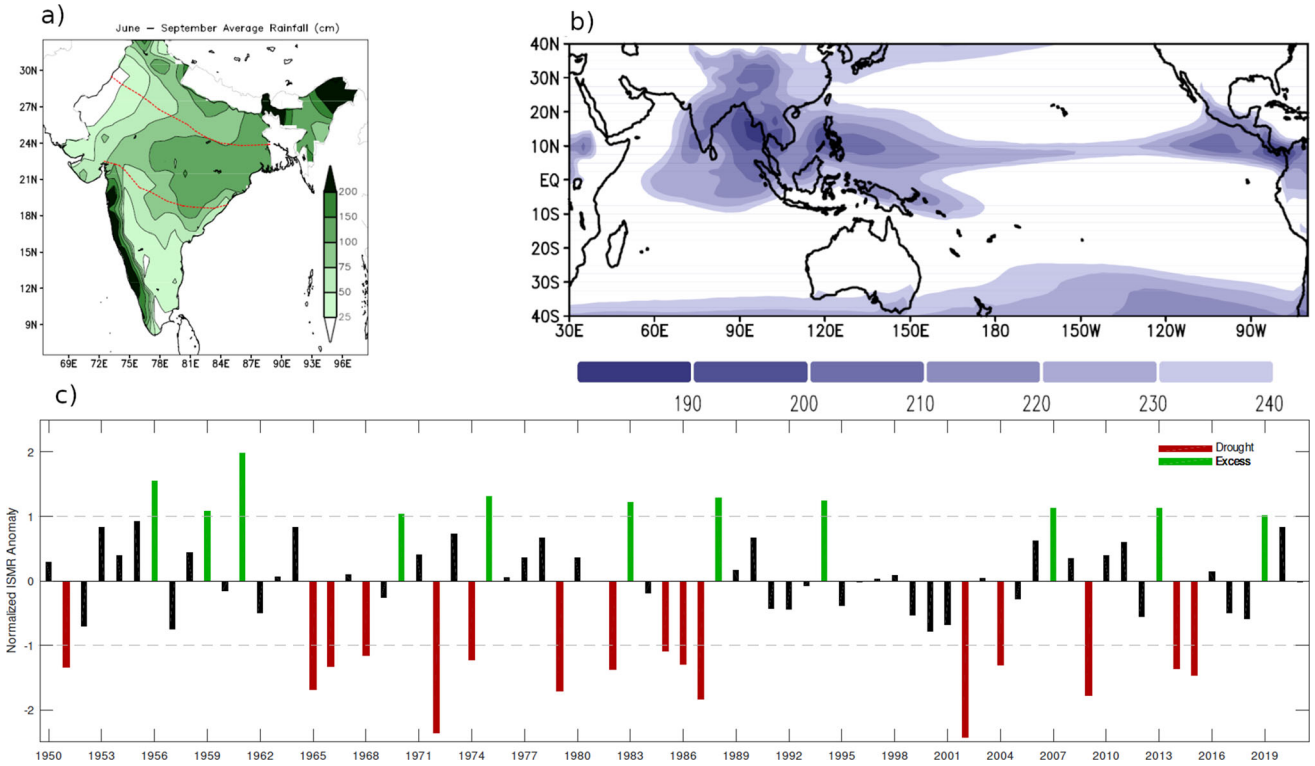

Figure 1. (**a**) June–September mean rainfall (cm), (**b**) the mean June–September OLR, and (**c**) variation of normalized ISMR anomaly during 1950–2020.

from the equatorial Indian Ocean and synoptic scale systems generated over the surrounding Arabian Sea and Bay of Bengal propagating onto the Indian region (Gadgil 2003 and references therein). Therefore, we expect the monsoon and monsoon variability to be linked to the variability of convection over some regions of the surrounding oceans and the Pacific. Here we focus on the component of monsoon variability contributed by convection over these oceanic regions.

We use an index of the summer monsoon rainfall over the Indian region, i.e., the all-India summer monsoon rainfall (ISMR), which is a weighted average of the June–September rainfall at 306 well-distributed rain gauge stations across India (Parthasarathy *et al.* 1994) available at https://www.tropmet.res.in/. One of the most important features of the monsoon variability is the interannual variation (figure 1c) of ISMR. Although the interannual variation is not large, with the standard deviation of about 10% of the mean, it has a large impact on Indian agricultural production and the overall economy (Gadgil and Gadgil 2006).

A major advance in our understanding of the interannual variation of the ISMR occurred in the eighties with the discovery of a strong link with ENSO (Sikka 1980; Rasmusson and Carpenter 1983). Sikka showed that the epochs of high/low frequency of the occurrence of El Niño events identified by Reiter (1978) on the basis of line-island precipitation index coincided with epochs of high/low frequency of monsoon droughts identified by Joseph (1976) and thereby gave support to the gospel since Sir Gilbert Walker that El Niño events (warm phase, low SOI) lead to deficient Indian monsoon rains, while La Niña events (cold phase high SOI) go with above average rainfall.

In this study of the association of ISMR with ENSO, we use an index for ENSO based on the Niño3.4 SST anomaly (https://cpc.ncep.noaa.gov/), since the simultaneous correlation coefficients between the SST of Niño3/Niño3.4/Niño4 and ISMR based on all the years between 1881 and 1998 are −0.57/−0.59/−0.47, respectively (Ihara *et al.* 2007). Kumar *et al.* (2006) have shown that the most notable difference in the tropical Pacific SSTs between the El Niño events associated with droughts and drought-free ones is the greater equatorial central Pacific warming during failed Indian monsoon years. Ihara *et al.* (2007) reached the same conclusion. These analyses suggest that India is more prone to drought when the ocean

warming signature of El Niño is large over the central equatorial Pacific. These results support our choice of Niño3.4 SST as the basis of the ENSO index. The warm phase of ENSO is known to be unfavourable for monsoon rainfall, whereas the cold phase is favourable for monsoon rainfall. *We define our ENSO index as the negative of the Niño3.4 SST anomaly normalized by the standard deviation, so that positive values of the ENSO index are associated with a cold phase of ENSO, i.e., the phase favourable for the monsoon.* Henceforth we will refer to all cold (warm) events as La Niñas (El Niños) as is commonly done in specifying prediction for the phase of ENSO.

The observed relationship between ISMR and ENSO for the period 1950–2020 is depicted in figure 2. The correlation of the ISMR and our ENSO index is positive and high. If we consider the years which are characterized by non-negligible values of the ENSO index and ISMR anomalies (i.e., the magnitude of the ENSO index greater than 0.1 and the magnitude of the ISMR anomaly greater than 0.2), 74% of the seasons with a negative ENSO index have a negative ISMR anomaly and 73% of the seasons with positive ENSO index have a positive ISMR anomaly. We have tested whether the monsoon–ENSO relationship, i.e., the association between the signs of the anomalies of the monsoon rainfall and ENSO index is significant (see Appendix). We find that the association of signs of ISMR anomalies and signs of the ENSO index over the entire range of variation of ENSO index, as well as of positive ISMR anomalies with positive ENSO index and negative ISMR anomalies with negative ENSO index are all statistically significant. This strong association between the seasonal rainfall anomalies and the ENSO index is the backbone of the popular gospel.

In order to study convection over the oceans, we have analyzed the OLR (Liebmann and Smith 1996) in the satellite era, 1982–2021. The relation of the ISMR anomaly with the seasonal ENSO index remains strong in this shorter period (correlation coefficient −0.51). However, the sample size of 1982–2021 is too small to test the statistical significance as was done for 1950–2020.

A key question in monsoon prediction is whether the summer monsoon rainfall will be deficient or above normal. Once the seasonal prediction of ENSO is available, the expected sign of the ISMR anomaly is readily deduced on the basis of the monsoon–ENSO relationship. However, it is widely

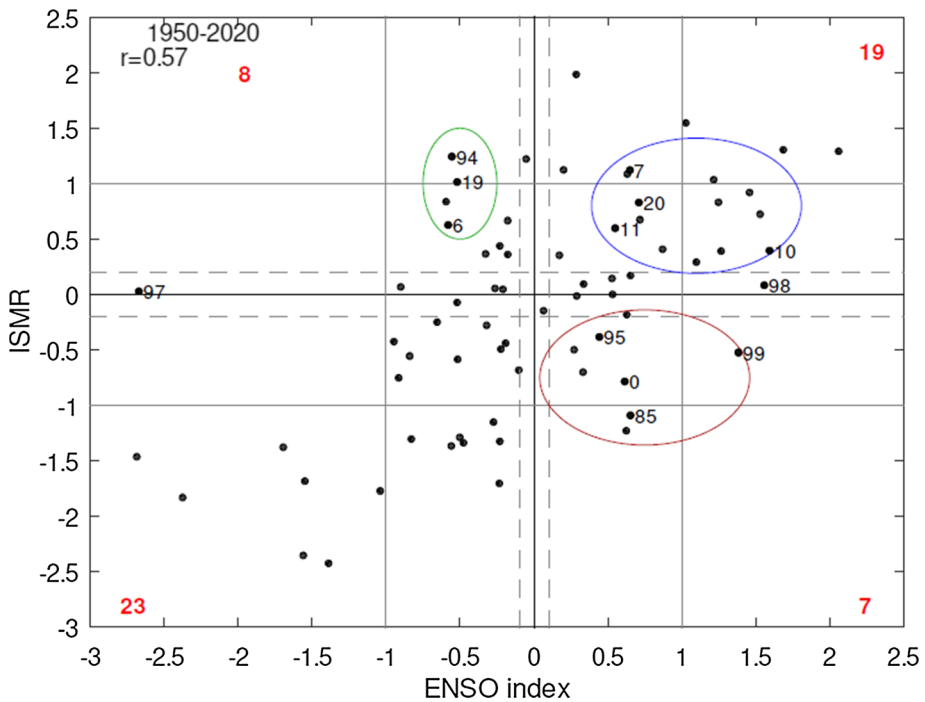

Figure 2. Variation of ISMR anomaly (normalized by the standard deviation) *vs.* the ENSO index during 1950–2020. The green curve is the boundary of exceptional cases of the cold phase of ENSO. The red curve is the boundary of the analyzed set of exceptional cases of the cold phase, i.e., 1985, 1995, 1999, 2000. The blue curve is the boundary of years with similar values of ENSO but with positive ISMR anomaly, i.e., 2007, 2019, 2011, 2020 chosen for comparison with this set of exceptional years.

known that there are exceptions (such as the drought during the La Niña of 1985) for which the sign of the ISMR anomaly predicted on the basis of this relationship is the opposite of what is observed. Here we attempt to supply an explanation for rogue La Niñas, i.e., ISMR deficits in cold ENSO phases, one that provides predictive skill beyond ENSO.

For La Niñas, the monsoon seasons which are characterized by negative signs of ISMR anomalies are surrounded by a red boundary in figure 2, whereas for El Niños, the monsoon seasons which are characterized by positive signs of ISMR anomalies are surrounded by a green boundary in figure 2. The problem of understanding the anomalous behaviour of the monsoon during the warm phase has received considerable attention and the exceptional cases have been attributed to a favourable phase of Equatorial Indian Ocean Oscillation, EQUINOO (Gadgil *et al.* 2004, 2020) and Indian Ocean dipole events (Saji *et al.* 1999; Webster *et al.* 1999; Ashok *et al.* 2001). Unfortunately, neither of these has yet been shown to be predictable.

So far, explaining the exceptional cases of deficient monsoon rainfall in the cold phase of ENSO has not been addressed, although they are a substantial fraction, i.e., 27% and 36% of the La Niña cases for the periods 1950–2020 and 1982–2021, respectively. A failure of the prediction for the La Niñas of the monsoon being above normal is likely to have a larger adverse impact than the false prediction of a deficit for the exceptional cases of El Niño. Here we will attempt to understand the exceptional La Niña cases which we call the rogue La Niña.

2. Relationship of ISMR and ENSO with convection over different parts of the Indo-Pacific oceans

For the period 1982–2021, figure 3 shows the spatial variation of the correlation of the ISMR with the OLR along with the correlation coefficients over representative regions of the Indian and Pacific Oceans. Convection over the Indian region, hence ISMR, is positively correlated with convection over the north Indian Ocean and equatorial Indian Ocean except for the eastern equatorial Indian Ocean (EIO). Convection of the monsoon system is maximum over the Bay of Bengal (figure 1), and a great deal has been written about the synoptic scale systems which propagate from the Bay onto the Indian region. Nonetheless, one can see in figure 3 that the variability of the monsoon rainfall is linked much more to the convection over the eastern Arabian Sea and the western equatorial Indian Ocean.

ISMR is negatively correlated with convection over the equatorial central Pacific which is a manifestation of the monsoon-ENSO link. Note that although the relationship of the ISMR anomaly with the equatorial central Pacific is believed to be the most important, the magnitude of the correlation coefficient of ISMR with the convection over the Arabian Sea is actually larger. The importance of convection over the Arabian Sea is clearly brought out in the comparison of the OLR anomaly patterns for the drought of 1987 and the excess rainfall season of 1988 (figure 4) which are canonical examples of a drought associated with El Niño and excess rain associated with La Niña. It is seen that the OLR anomaly pattern of the season

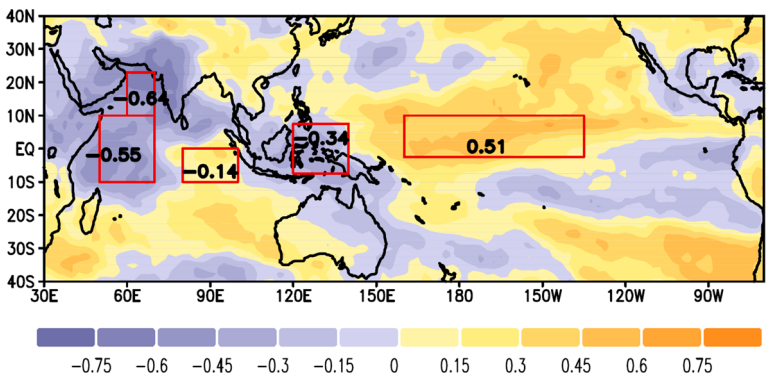

Figure 3. Map of correlation coefficients of ISMR with June–September mean OLR. Representative regions – Arabian Sea (60°–70°E, 10°–23°N), West equatorial Indian Ocean (WEIO, 50°–70°E, 10°S–10°N), East equatorial Indian Ocean (EIO, 80°–100°E, 10°S–EQ), equatorial West Pacific (120°–140°E, 7.5°S–7.5°N).

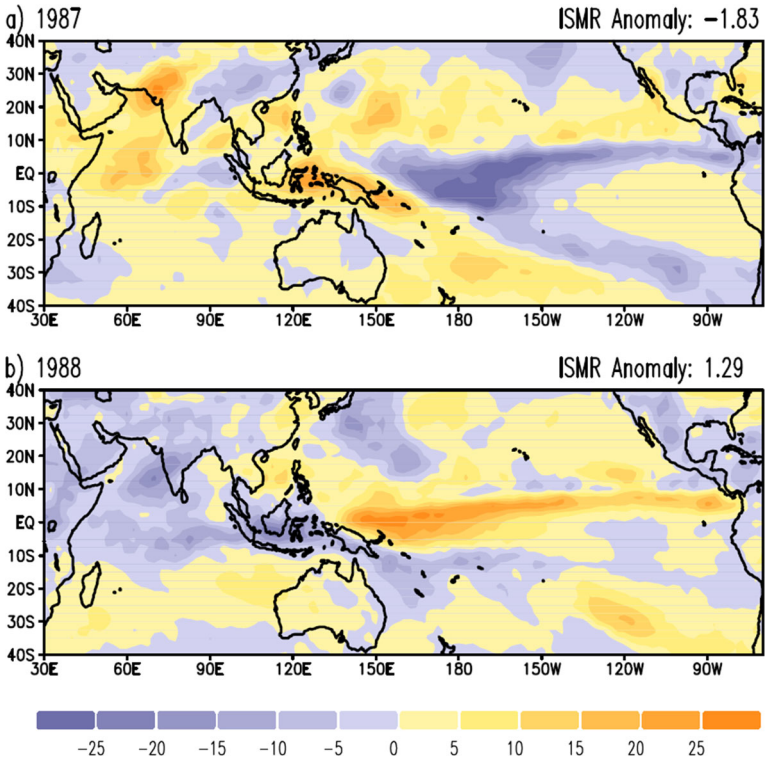

Figure 4. June–September mean OLR anomalies for the (**a**) drought of 1987 and (**b**) excess monsoon season of 1988.

with ISMR well above normal is characterized by intensification of convection over the Arabian Sea and western equatorial Indian Ocean. On the whole, there is weaker intensification of convection over the Bay of Bengal. Consistent with this, the season with deficit ISMR is characterized by suppressed convection over the Arabian Sea and western equatorial Indian Ocean, and relatively less suppression over the Bay.

The prominent feature of the mean SST of the Arabian Sea and the western equatorial Indian Ocean is the cold SST off the coast of East Africa due to upwelling. Izumo *et al.* (2008) have studied the impact of the upwelling region on the summer monsoon rainfall over the Indian region and shown that a decrease in the upwelling leads to an increase in the rainfall over the west coast of India. Vecchi and Harrison (2004) find that the rainfall over the west coast during June–July is positively correlated with the SST of the northern Arabian Sea, extending from the upwelling region to the west Coast. In September–October, the rainfall is correlated with the SST of the eastern Arabian Sea and western equatorial Indian Ocean. Our focus is on the Indian summer monsoon rainfall for which the important convective part of the Arabian Sea is to the north of the equatorial belt and east of the upwelling region off the Somali coast. That is the part of Arabian Sea which we refer to as the Arabian Sea in this paper.

3. Understanding rogue La Niñas

The aim of the following analysis is to identify critical regions which contribute to the observed negative ISMR anomaly in rogue La Niña years. The approach we adopt is as follows. We consider first the impact of ENSO on the rainfall over the Indian region, which can be a direct response to the variation of convection over the equatorial central Pacific as envisaged in the Walker circulation, or indirectly, by altering convection in regions of the Indo-Pacific that can impact rainfall over India.

The spatial variation of the correlation with ENSO index of the OLR over the Indian and Pacific Oceans with the correlation coefficients in regions which are well correlated, is shown in figure 5. We note that over all of the Indian Ocean, and the equatorial West Pacific, the correlation of ENSO index with OLR is negative. Thus we expect that, on average, ENSO-triggered OLR anomaly for the cold phase is negative (i.e., convection is enhanced) over this entire region. In fact, it turns

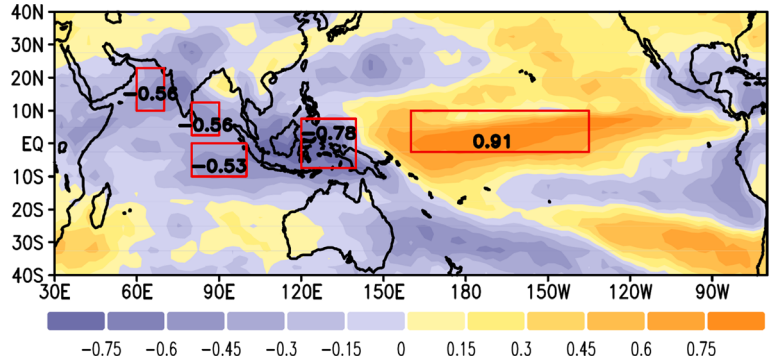

Figure 5. Map of correlation coefficients of June–September mean ENSO index with June–September mean OLR.

out that over these oceanic regions, in the composite of all years with ENSO index positive, the OLR anomaly is negative and in the composite of all years with ENSO index negative, the OLR anomaly is positive (figure not shown). Thus positive ENSO index is generally associated with enhanced convection over these oceanic regions. An enhancement of convection over almost the entire Indian Ocean is associated with an enhancement of ISMR (compare figures 3 and 5). As envisioned in the Walker circulation, the descent over the equatorial central Pacific during La Niña leads to ascent to the west over the region comprising the western equatorial Pacific, the Indian Ocean and the Indian region. The notable exception is for the eastern equatorial Indian Ocean (EIO, 80°–100°E, 10°S–EQ), for which a negative OLR anomaly being triggered by the cold phase of ENSO implies a decrease of ISMR.

The overall impact of ENSO on monsoon rainfall depends on the outcome of the tug of war between the impact of the convection anomalies over the EIO and the impact of convection anomalies over the rest of the north and equatorial Indian Ocean, with the latter generally dominant (cf. figure 4).

Over most of the regions, for most of the years, the OLR anomaly triggered by positive ENSO index leads to positive ISMR anomaly and that triggered by negative ENSO index to negative ISMR anomaly; i.e., to the canonical monsoon–ENSO relationship. The red and green boundaries in figure 2 encircle the exceptional years in which the sign of the ISMR anomaly is opposite to that of the ENSO index. In the satellite era from 1982 to 2021, the prominent exceptional cold phase years when the ISMR anomaly is negative, despite the ENSO index being positive are 1985, 1995, 1999 and 2000. The warm phase years 1994, 2019 and 2006 are exceptional years when the sign of the ISMR anomaly is

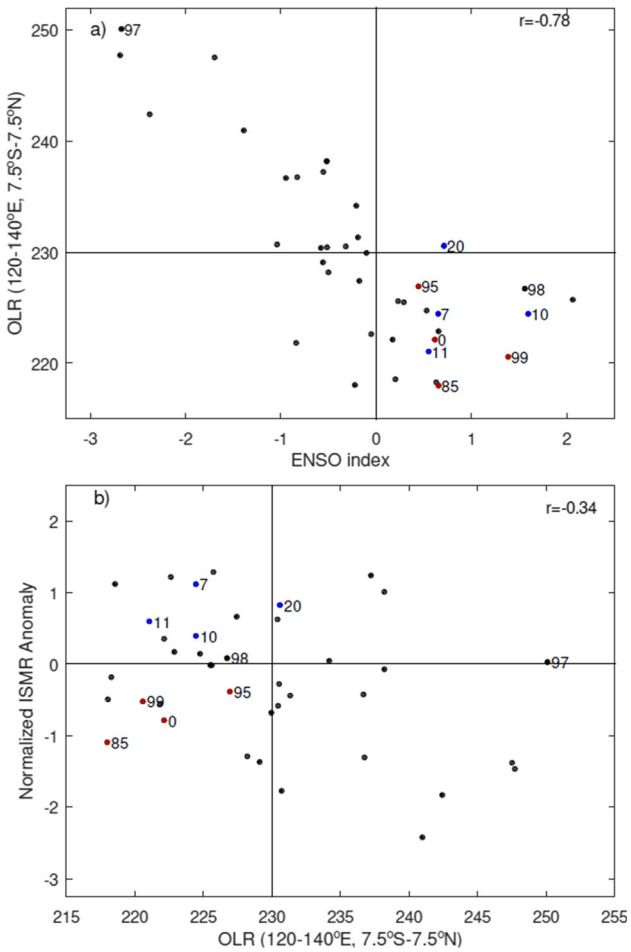

Figure 6. Scatter plots for equatorial West Pacific (120°–140°E, 7.5°N–7.5°S) of June–September mean (**a**) OLR *vs.* ENSO index and (**b**) ISMR anomaly *vs.* OLR. The red points are rogue La Niñas and blue, years chosen for comparison with similar ENSO values but positive ISMR anomaly.

positive. Canonical predictions of above-normal rainfall in the cold phase and below-normal rainfall for the warm phase, are totally wrong for these exceptional years. In order to unravel the factors leading to the observed ISMR anomalies in

exceptional years in the cold phase, we examine the OLR observations. We will contrast the rogue La Niña years with similar ENSO values characterized by positive ISMR anomalies, i.e., 2007, 2010, 2011 and 2020.

We consider the regions over which the OLR is well correlated with ENSO index (figure 5). The region with the highest correlation is the equatorial central Pacific, at the heart of ENSO. The next, the far western Pacific and Maritime Continent, is also an intrinsic part of ENSO and has opposite sign; there is greater ascent in this region when there is greater descent over the central Pacific (i.e., in the cold phase). Scatter plots depicting variation of OLR over the equatorial West Pacific with ENSO index and the variation of the ISMR anomaly with the OLR over this region are depicted in figure 6. In the scatter plots, the exceptional years of the cold phase are marked in red and the years in the set chosen for comparison are characterized by positive ISMR anomalies, marked by blue (figure 6). It is seen that the relationship of the OLR anomaly over the western equatorial West Pacific with ENSO is very strong. This is a manifestation of the ascent over the equatorial central Pacific, leading to descent to the west.

The OLR over this region for the set of rogue La Niñas is very low and lower than those with similar ENSO values which were observed to be characterized by positive ISMR anomalies. Thus, the OLR over this region for the exceptional cases of cold events is expected to contribute to the enhancement of ISMR and hence contribute towards the canonical ENSO–monsoon relationship.

We find that the ENSO-triggered OLR anomaly for some other regions such as the southwest Bay of Bengal also contributes to the canonical ENSO–monsoon relationship. The exceptional regions are the Arabian Sea and the EIO.

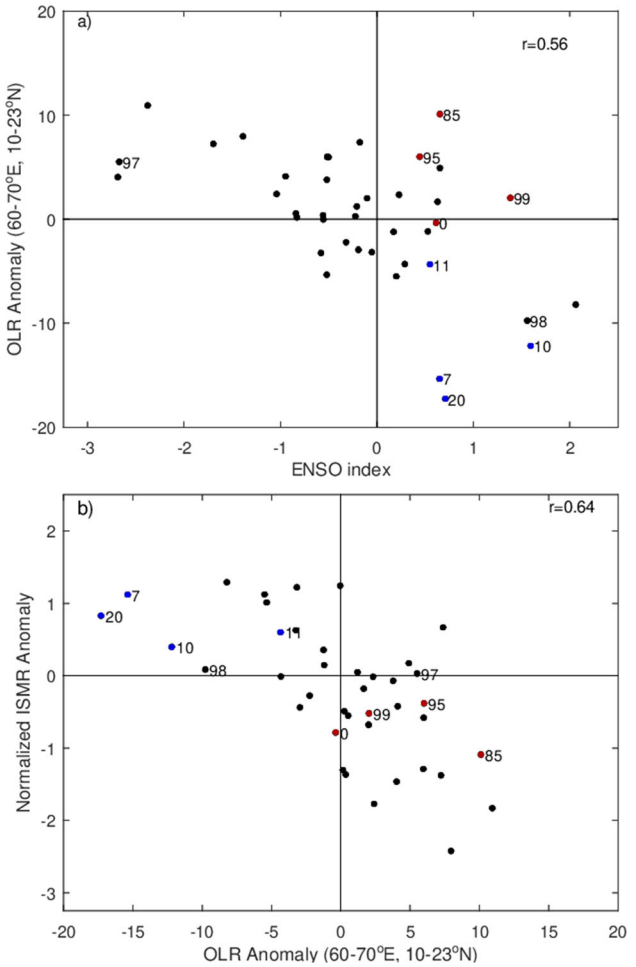

Figure 7. Scatter plots as in figure 6, but for Arabian Sea (60°–70°E, 10°N–23°N) of (**a**) OLR anomaly *vs.* ENSO index and (**b**) ISMR anomaly *vs.* OLR anomaly.

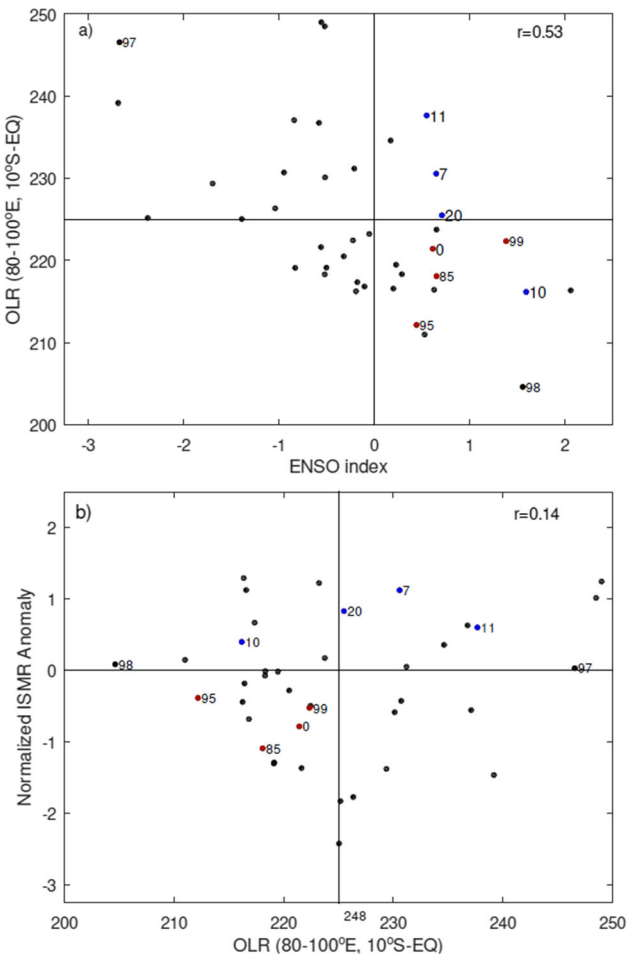

Figure 8. Scatter plots as in figure 6, but for equatorial eastern Indian Ocean (80°–100°E, 0°–10°S) of (**a**) OLR *vs.* ENSO index and (**b**) ISMR anomaly *vs.* OLR.

3.1 *Arabian Sea*

The relationship of the OLR over this region with ENSO index and of the OLR anomaly with the ISMR anomaly is depicted in figure 7(a and b), respectively. The OLR over this region is highly correlated with ENSO index; the strong El Niño of 1997 is associated with high OLR and the strong La Niña of 1998 with low OLR. However, despite the ENSO index being positive, for three of the four exceptional cold events (1985, 1995, 1999), the OLR anomaly over this region is positive and for 2000 it is very small. This is an anomalous response to the positive ENSO phase. This implies that the OLR over this region of this set is associated with a negative ISMR anomaly. So the Arabian Sea is a critical region for the set of exceptional cases of cold phase ENSO with a negative ISMR anomaly.

The high correlation of OLR over this region with ISMR anomaly is manifested in the sign of the ISMR anomaly being the same as that of the OLR anomaly in a vast majority of the years (37 out of 40) including three of the four rogue La Niña years. Thus, the convection over the Arabian Sea is strongly connected to the interannual variation of the monsoon rainfall.

3.2 *Eastern equatorial Indian Ocean*

We note that suppression (enhancement) of convection over the EIO is associated with increase (decrease) of ISMR (figure 3). Over the EIO, although the correlation with ISMR is small when all ENSO events are considered, the OLR anomaly is negative for all the rogue La Niñas (figure 8). So the variation of the OLR anomaly in the eastern equatorial Indian Ocean also aligns with the negative ISMR anomaly for the set of exceptional cases in the cold phase of ENSO.

Thus the two regions over which the OLR anomaly variations in the cold phase of ENSO contribute to negative ISMR anomaly are the Arabian Sea and the Eastern Equatorial Indian Ocean. Hence these are critical regions for exceptional cases of cold phases.

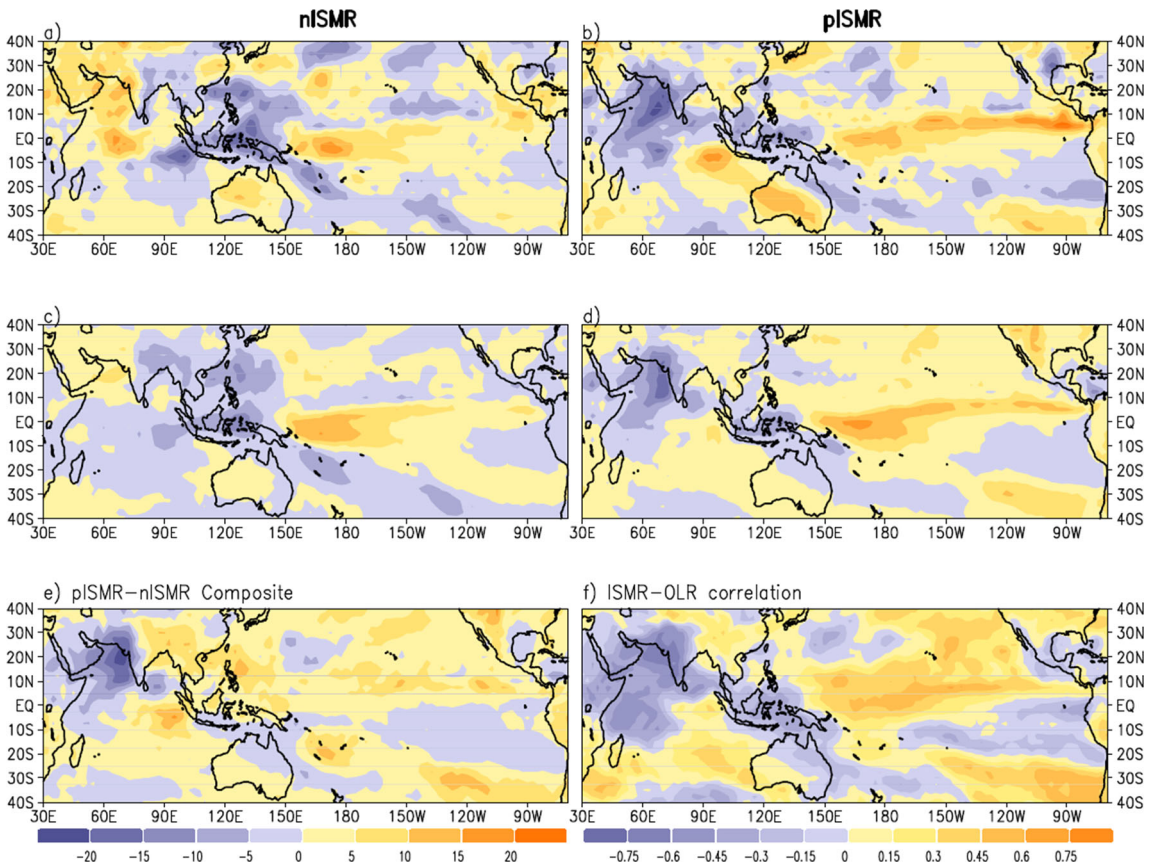

Figure 9. OLR anomaly for June–September (**a**) 1985, (**c**) composite of 1985, 1995, 1999, 2000 (nISMR) and (**b**) 2007, (**d**) composite of 2007, 2010, 2011, 2020 (pISMR), (**e**) difference between pISMR and nISMR composites, and (**f**) correlation of ISMR with OLR.

3.3 *Variation in convection patterns*

We next consider the JJAS OLR patterns over the entire Indo-Pacific region for (2007, 2010, 2011, 2020), the normal cold phase years associated with positive ISMR anomalies (pISMR), and for (1985, 1995, 1999, 2000), the exceptional cold phase years with negative ISMR anomalies (nISMR). Figure 9 shows OLR anomalies for: (a) the nISMR year 1985; (b) the pISMR year 2007; (c) the composite of the OLR anomalies of all nISMR years; and (d) the composite of the OLR anomalies of all pISMR years. The difference between the composites of the nISMR and pISMR years is shown in figure 9(e).

The major differences in the OLR anomaly patterns of the pISMR and nISMR years are again seen to be over (i) the Arabian Sea, north of 10°N and west of 60°E and (ii) the eastern equatorial Indian Ocean (EIO). These two regions are well correlated with ENSO index, but the OLR anomalies over each of these regions are of opposite signs for pISMR and nISMR. Of these, convection over the Arabian Sea is enhanced whereas that over the EIO is suppressed in the OLR anomaly composite of pISMR *vis-a-vis* nISMR (figure 9e).

The correlation of ISMR with OLR is shown in figure 9(f). The similarity of the composite pattern of pISMR and the correlation of ISMR with OLR is striking. There is one noteworthy feature about the OLR anomaly over the Indian region characterizing the nISMR composite. The OLR anomaly over the northwestern part of the monsoon zone is positive as expected when the ISMR anomaly is negative. However, the OLR anomaly over the eastern part of the monsoon zone is negative and this band of negative OLR anomaly stretches to 150°E in northwest tropical Pacific. This pattern has been referred to as the Indian rainfall dipole by Izumo *et al.* (2008) in their study of the impact of Arabian Sea upwelling. On the other hand, the negative OLR anomaly over the monsoon zone in pISMR years tends to extend over almost the entire monsoon zone in most cases as well as in the composite.

4. Role of the critical regions in interannual variation of ISMR

The correlation between the OLR over the Arabian Sea and the EIO is very poor: $r = 0.06$ for the period 1982–2021. This implies that if they are considered together, the impacts of the convection over these regions on ISMR would add. This leads

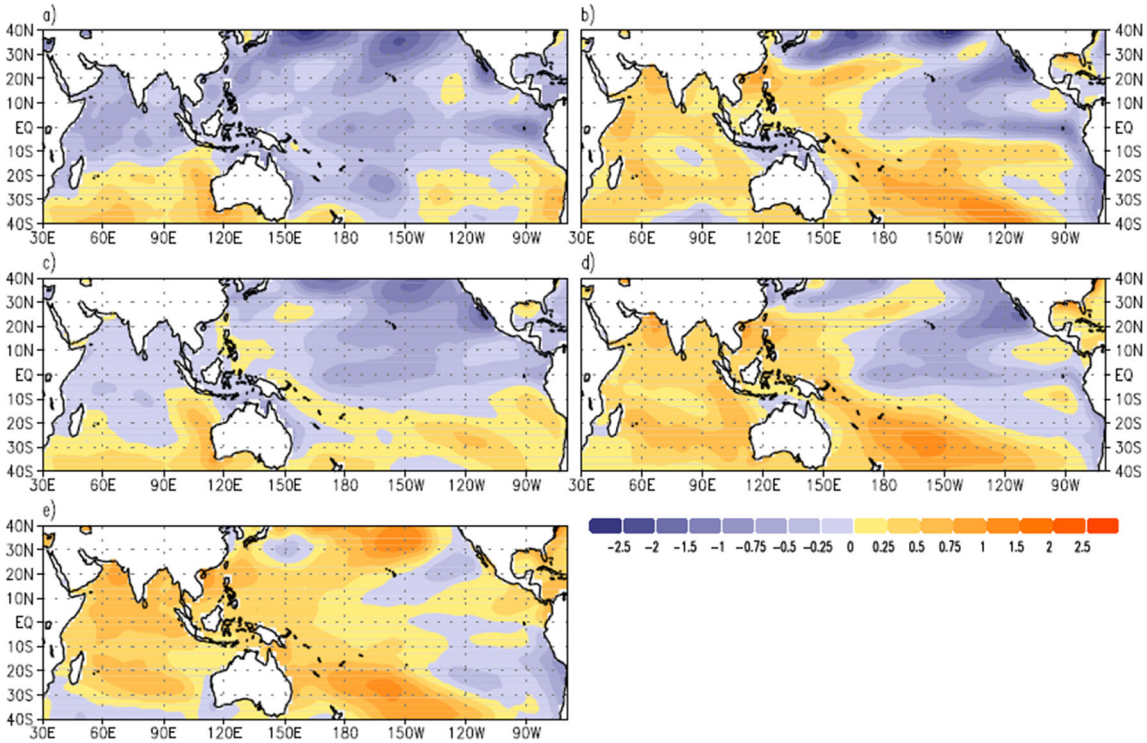

Figure 10. For June–September. (**a**) SST anomaly for 1985, (**b**) SST anomaly for 2007, (**c**) SST anomaly of the composite of nISMR 1985, 1995, 1999, 2000, (**d**) SST anomaly for composite of pISMR 2007, 2010, 2011, 2020, and (**e**) difference in SST anomaly composites of pISMR and nISMR.

to the small magnitude of the ISMR anomaly in 1997 in which the highly favourable convection over EIO balances the highly unfavourable convection over the Arabian Sea (figures 7 and 8). Another example is the strong La Niña of 1998 for which the highly favourable convection over the Arabian Sea balances the highly unfavourable convection over EIO (figures 7 and 8). This suggests that the OLR over each of the two regions and the total impact of the OLR over these two regions are important factors determining ISMR.

We find that almost all the seasons with excess rainfall or above-normal rainfall are characterized by negative OLR anomaly over the Arabian Sea. On the other hand, almost all the seasons with below-normal rainfall or droughts are characterized by positive OLR anomaly over the Arabian Sea. If we consider only La Niñas, we find that all the seasons with excess rainfall or above normal rainfall are characterized by negative OLR anomaly over the Arabian Sea and all seasons of droughts or below normal rainfall are characterized by positive OLR anomaly over the Arabian Sea. Thus convection over the Arabian Sea plays a critical role in the interannual variation of the monsoon.

5. Understanding the variation of convection over the Arabian Sea

Since we have been looking at the variation of convection over a tropical ocean, we will first check whether the variability of convection over the Arabian Sea is related to the variability of the SST.

The SST anomaly for 1985 from the set of exceptional cases (nISMR) and for the composite of the set are compared with the SST anomaly for 2007 (pISMR) of the set chosen for comparison and for the composite of that set in figure 10. We used NOAA extended reconstructed SST (ERSST, Huang *et al.* 2017) in this study. It is seen that the SST anomaly of the exceptional cases (nISMR) is negative over a large part of the north Indian

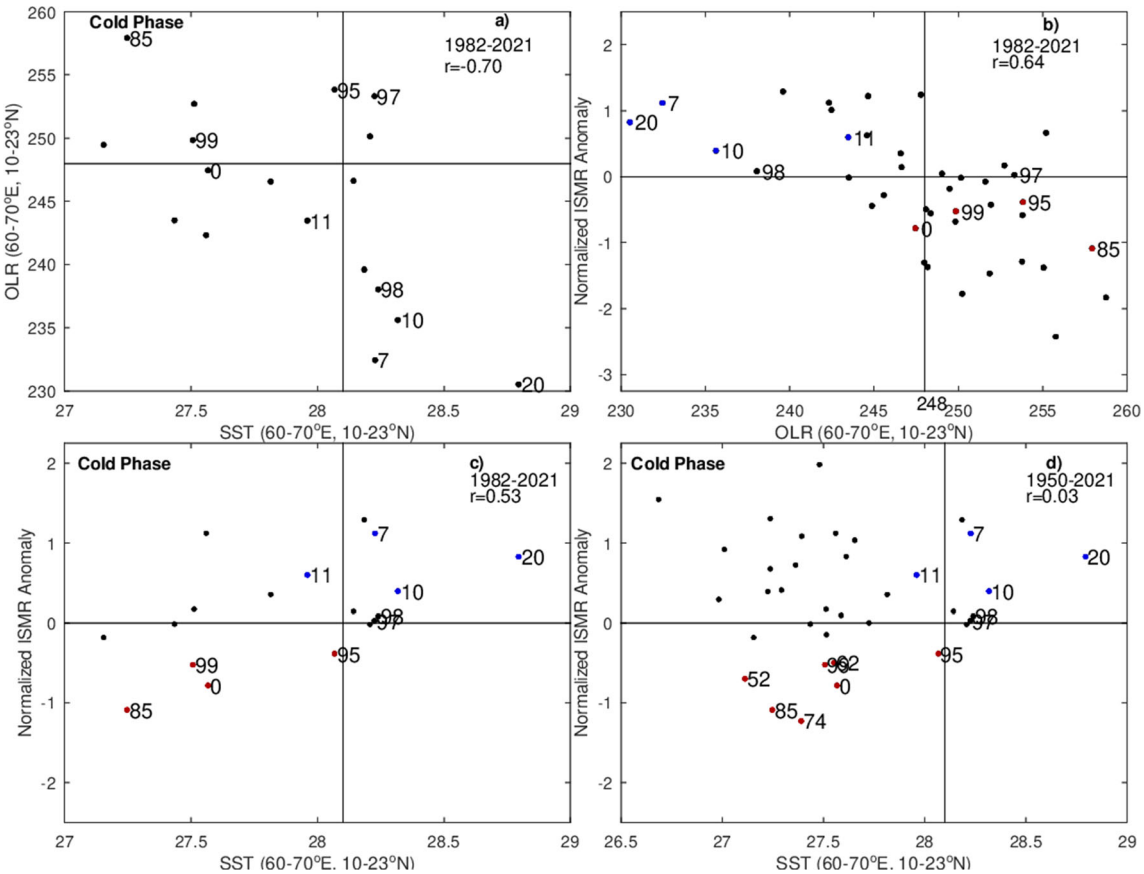

Figure 11. For cold phase during 1982–2021, scatter-plot of (**a**) OLR over the Arabian Sea *vs.* SST of the Arabian Sea; (**b**) ISMR anomaly *vs.* OLR over the Arabian Sea, (**c**) ISMR anomaly *vs.* SST of the Arabian Sea, and (**d**) for 1950–2021 ISMR anomaly *vs.* SST of the Arabian Sea.

Ocean including the Arabian Sea, whereas SST anomaly is positive for the other set of seasons (pISMR). This is also well brought out in the difference between the SST anomalies of the composites (figure 10e). Thus enhancement of convection over the Arabian Sea is associated with increase in the SST. We expect to find such a relation based on earlier studies of the relationship between SST and convection over the tropical oceans (Gadgil *et al.* 1984; Graham and Barnett 1987), which showed that there is a threshold SST across which the mean convection increases with SST and above which the propensity for convection is high.

For the cold phase of ENSO index, we consider the relationship of ISMR with Arabian Sea OLR (figure 11a), that of Arabian Sea OLR with Arabian Sea SST (figure 11b), and ISMR with Arabian sea SST (figure 11c) for 1982–2021. Since ISMR is highly correlated with OLR over the Arabian Sea, ISMR is also well correlated to the SST of the Arabian Sea. Also, for this sample of years, when SST is below 28.1°C, there is a large range over which ISMR varies from −1.1 to +1.2 and there are several exceptional cases. However, when SST is above 28.1°C, there are no exceptional cases. *This is an important input for prediction, because it implies that when ENSO index is predicted to be positive and when the Arabian Sea SST is above this threshold of 28.1°C, the ISMR is either normal or above normal.*

The analysis so far was restricted to the period 1982–2021 because it also involved the analysis of OLR. The period 1982–2021 is marked by increasing global temperature, and all the exceptional cases fall in the first half of the period while the normal cases are mostly in the second half. Hence it may be argued that our result is not indicative of the importance of convection in the Arabian Sea, but is a consequence of greater global warming. We can rule this out by looking at the observational record from 1950 for SST.

Consider the variation of ISMR with SST for this longer period (figure 11d). The correlation between ISMR and SST for this longer period is poor. However, the relationship for high SSTs turns out

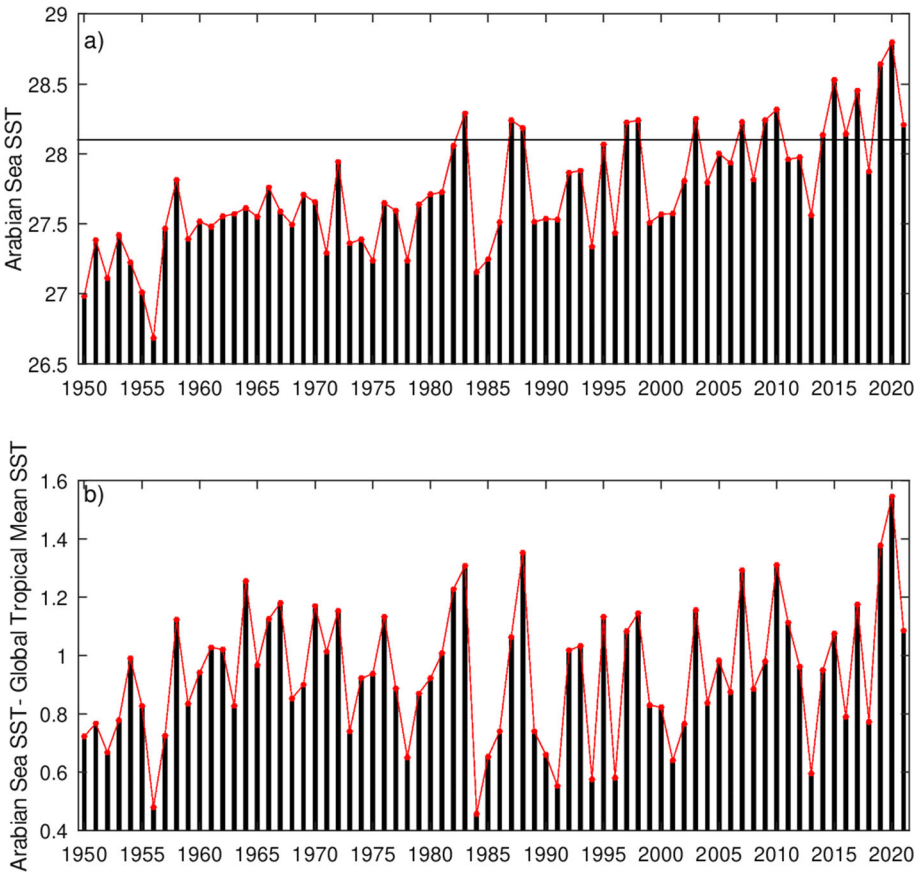

Figure 12. (**a**) Variation of June–September mean SST of Arabian Sea (60°–70°E, 10°–23°N) during 1950–2021. The horizontal line representing SST equal to 28.1°C is also shown. (**b**) Variation of the difference of June–September SST of Arabian Sea and the global tropical mean SST (20°S–20°N, 0°–360°E) during 1950–2021.

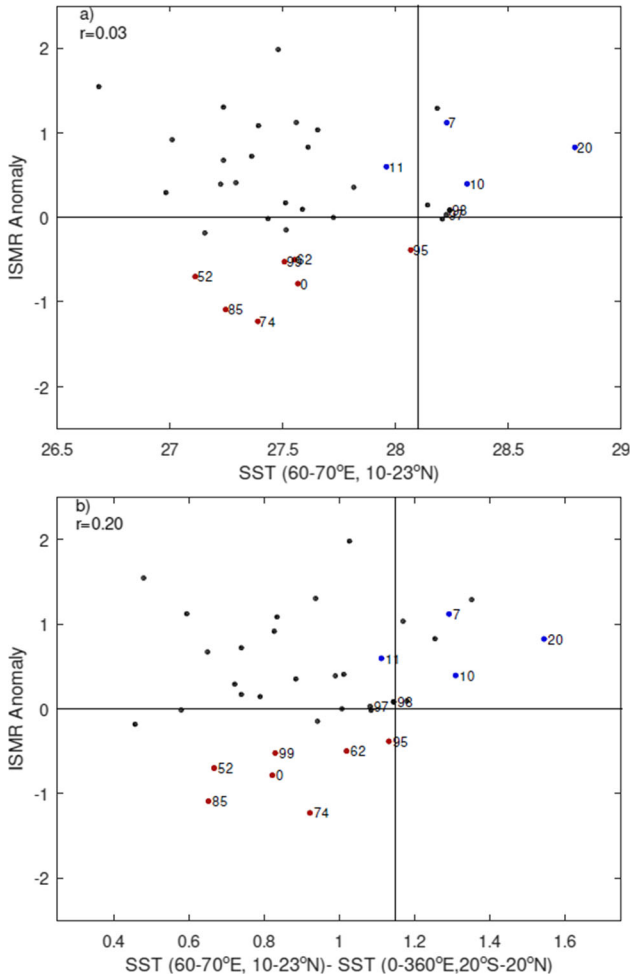

Figure 13. Scatter plot of ISMR anomaly. (**a**) SST of the Arabian Sea and (**b**) difference between SST and the tropical mean SST (20°S–20°N, 0°–360°E) for the cold phase of ENSO in the period 1950–2021.

to be identical to that derived for the smaller dataset. Again, when SST is below 28.1°C, there is a large range over which ISMR varies from −1.2 to +2. Note that there are several exceptional cases before 1982, meaning that rogue La Niñas have occurred in this period when SST is below 28.1°C, However, when SST of the Arabian Sea is above 28.1°C, there are no rogue La Niñas. *The prediction that SST > 28.1°C is important because it implies that when the ENSO index is predicted to be positive, the ISMR is either normal or above normal.*

6. Understanding of the warming of the Arabian Sea in certain years

Variation of the Arabian Sea SST during 1950–2021 is shown in figure 12(a). There is a clear warming trend, as expected with increasing greenhouse gases. Consequently, the propensity for SST > 28.1°C is high after the mid-eighties and particularly high in the 21st century, though not all recent years have SSTs above 28.1°C. Thus there could be an impact of global warming in preventing monsoon rainfall deficits over the Indian region during the cold phase of El Niño. The secular SST warming trend of the Indian Ocean is greater than most of the tropical Pacific and Atlantic, especially since the 1950s. The warming trend is particularly high over the eastern Arabian Sea and the West equatorial Indian Ocean (Sun *et al.* 2019). The existence of the warming trend of the Arabian Sea as well as the global warming trend are found to be statistically significant at 5%.

Convection over the tropical oceans depends on SST and moist static stability. Observations show that there is an adjustment of upper tropospheric temperatures in response to SST which leads to a close co-variability between SST threshold and tropical mean temperature (Johnson and Xie 2010). Hence tropical precipitation changes are positively correlated with spatial deviations of SST warming from the tropical mean (Xie *et al.* 2010). The variation of the deviation of SST from the tropical mean during 1950–2021 is shown in figure 12(b). The Arabian Sea SST is observed to be higher than the global mean throughout the period. This implies that the global change will be reflected as 'warmer-gets-wetter' (increased rainfall where the rise in sea surface temperature (SST) exceeds the mean surface warming) pattern. The minimum SST anomaly for no rogue La Niñas is 1.18°C (figure 13).

Even when the propensity of high SST is high, in the latter part of 1950–2020, the SST is lower than 28.1°C for La Niña years such as 2000 and 2013 (figure 13). So it is necessary to predict whether the SST will be higher than 28.1°C for each year for predicting that there will not be any rogue La Niñas.

7. Prediction of Arabian Sea JJAS SST

Since SST evolves more slowly than the atmospheric parameters, we next explore whether it is possible to predict June–September mean SST from the SST of the pre-monsoon season. The variation of June–September SST with April–May SST for 1950–2021 is shown in figure 14. The correlation is high. If the SST of April–May is sufficiently high (>29.6°C), the JJAS SST is greater than 28.1°C.

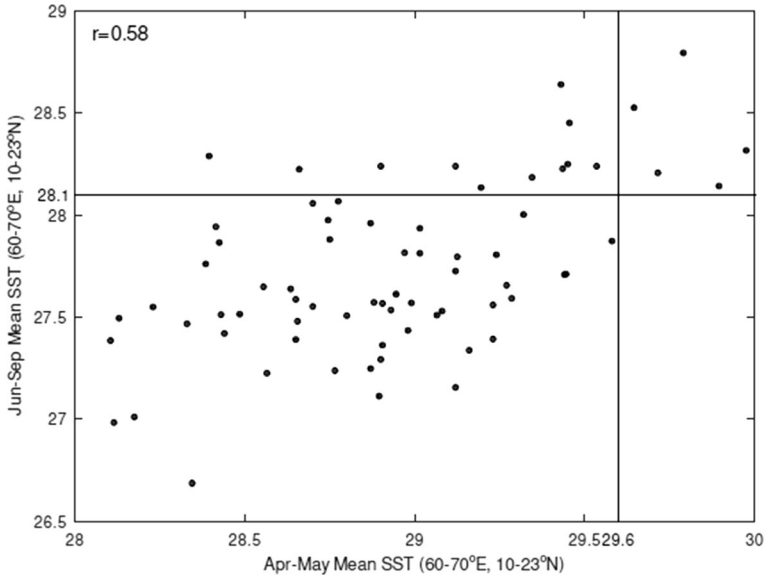

Figure 14. Scatterplot of JJAS mean SST of the Arabian Sea *vs.* April–May mean SST of the Arabian Sea.

Thus we conclude that if the Arabian Sea April–May SST is above 29.6°C, the June–September mean SST will be above 28.1°C and rogue La Niñas will not occur. We can then expect the monsoon–ENSO relationship for the cold phase will be the canonical one.

8. Conclusions

This analysis of OLR during 1982–2021 showed that ENSO has association with convection over large parts of the north Indian Ocean, equatorial Indian Ocean and the tropical Pacific Ocean. This ENSO-triggered convection over the oceans contributes to variation of ISMR, the strongest impact being with the convection over the part of the Arabian Sea east of the upwelling region along the coast of Africa and north of the equatorial belt. In fact, the convection over the Arabian Sea is better correlated with ISMR than the convection over the central equatorial Pacific corresponding to the monsoon–ENSO link.

The well-established monsoon–ENSO link with below-normal ISMR in the warm phase of ENSO and above-normal ISMR in the cold phase is the basis of most monsoon predictions. However, there are exceptions to this with some years in the cold phase with below monsoon rainfall and some in the warm phase with above monsoon rainfall. Our analysis of the exceptions in this link in the cold phase of ENSO – the rogue La Niñas, has identified the regions over which the OLR anomalies contribute to negative ISMR anomalies. These critical regions are the Arabian Sea and the eastern equatorial Indian Ocean (EIO). Rogue La Niñas are characterized by suppression of convection over the Arabian Sea and enhancement of convection over EIO, with the convection over the Arabian Sea playing a more important role. The positive OLR anomaly over the Arabian Sea is an anomalous response to the cold phase of ENSO.

For 1982–2021, we find that suppression of convection over the Arabian Sea characterizing rogue La Niñas is associated with a decrease in the SST of the Arabian Sea. Analysis of the SST of the Arabian Sea for this period, as well as 1950–2021, shows that while the chance of a negative anomaly of ISMR is comparable to that of positive ISMR anomalies in the colder range of SSTs, there are no rogue La Niñas at all when SST is above 28.1°C and the relationship of monsoon to ENSO is the canonical one. Arabian Sea is a region with a rapid warming trend with global warming. Hence the propensity of sufficiently high SST has increased in recent decades and the frequency of rogue La Niñas is expected to decrease.

We have shown that chance of nonoccurrence of rogue La Niñas, i.e., whether the SST of the Arabian Sea during June to September is above the critical value of 28.1°C, depends on whether the Arabian Sea SST in April–May is higher than 29.6°C. Thus it is possible to predict the chance of occurrence of rogue La Niñas from the April–May SST itself.

We have identified a feature that adds predictive skill to monsoon forecasts, but has less to say about its physics. We hypothesize that convection in the Arabian Sea is a control on the monsoon, driving

variations in atmospheric circulation that alter monsoon rainfall. The fact that the high SSTs needed for convection are prefigured in April–May, before the monsoon begins, supports this view. More work is needed to further support this hypothesis and fully rule out the possibility that the variations in the Arabian Sea are not so much a cause of monsoon failure but a corollary caused by something else.

Acknowledgements

It is a pleasure to acknowledge discussions with Dr M Rajeevan, Profs. J Srinivasan, P Vinayachandran and Dr S Sajani at different stages of this research. We also thank NOAA, USA (https://www.cdc.noaa.gov) for making the OLR and SST datasets used in this study and the Indian Institute of Tropical Meteorology, Ministry of Earth Sciences (https://tropmet.res.in) for providing All India Summer Monsoon Rainfall data for public access. MAC is supported by NSF grant OCE-2219829. The figures used in this article are prepared using GrADS and GNU Octave.

Author statement

All the authors contributed to the development of the research concept. Most part of the article is written by SG. Analysis of the data is done by PF and SG. SG, MAC and PF contributed to the interpretation of the results.

Appendix: ENSO–Monsoon associations

Siddhartha Gadgil[1] and Sulochana Gadgil[2]

[1]*Department of Mathematics, Indian Institute of Science, Bangalore.*
[2]*Centre for Atmospheric and Oceanic Sciences, Indian Institute of Science, Bangalore.*

The following text and analysis are available as a Jupyter notebook on Google Colaboratory at https://drive.google.com/file/d/1tBu6btHHZb5BL9CjGTxU9yFNkJx4H7dl/view?usp=sharing.

Questions

We investigate whether for the monsoon season as a whole, is there an *association* between ENSO index and rainfall. To do this, we compare with the appropriate null hypothesis using appropriate distributions and compute p values.

Null hypothesis and distributions/tests

To test for *association*, we take the null hypothesis to be that the signs of the ENSO index and rainfall anomaly are independent. We use the *Fisher exact test.*

We use scipy, specifically Fisher's exact test.

Import scipy.stats as stats.

Functions for p values

For the monsoon season, we have input a 22 matrix of frequencies, and we calculate three different p values, those for independence and for binomial on the right and left (with appropriate direction). For neatness, we capture all these in a single function, which returns these as percentages. Concretely, we return a triple with independence, positive ENSO and anomaly, and negative ENSO and anomaly.

```
from scipy.stats import binom

def assoc_percent_values(mat):
    odds, indep_p = stats.fisher_exact(mat)
    pos_p = binom.cdf(mat[1][1], mat[1][1] + mat[0][1], 0.5)
    neg_p = binom.cdf(mat[0][0], mat[0][0] + mat[1][0], 0.5)
    return indep_p * 100, pos_p * 100, neg_p * 100
```

We shall also return raw values, since we wish to correct for *multiple hypotheses*, i.e., cherry-picking statements that show stronger effects.

```
def assoc_p_values(mat):
    odds, indep_p = stats.fisher_exact(mat)
    pos_p = binom.cdf(mat[1][1], mat[1][1] + mat[0][1], 0.5)
    neg_p = binom.cdf(mat[0][0], mat[0][0] + mat[1][0], 0.5)
    return indep_p * 100, pos_p * 100, neg_p * 100
```

We now correct for cherry-pick. We have chosen whether to consider positive or negative associations after looking at the data. The general correction to the p-value is to observe that if we compute the probability q of an event X occurring, the p-value is not q but the probability of at least one of k independent events $X_1, \ldots, X_k$ occurring, with each having probability q. This probability is

$$p = 1 - (1 - q)^k$$

We define a function

```
def corrected(p, k):
  return 1.0 - ((1.0 - p) ** k)
```

Since we like to deal with percentages, it will be convenient to directly correct these.

```
def percent_corrected(p, k):
  return corrected(p/100, k) * 100
```

Computations

We test associations for total rainfall, and the positive and negative cases.

```
assoc_percent_values([[8, 19], [23, 7]])
```

```
(0.05200349105358732, 1.4479637145996094, 0.5336920265108347)
```

Results

- The clear conclusion is that there is a *significant* association, since the p-value is 0.05% and there are no multiple hypotheses.
- Both sides are well below 5%. Since this applies to both sides, no cherry-picking was involved, so we can conclude associations for both negative and positive ENSO for the conventional threshold of 5%.

References

Ashok Karumuri, Guan Zhaoyong and Yamagata Toshio 2001 Impact of Indian Ocean dipole on the relationship between the Indian monsoon rainfall and ENSO; *Geophys. Res. Lett.* **28**, https://doi.org/10.1029/2001GL013294.

Gadgil Sulochana 2003 The Indian monsoon and its variability; *Ann. Rev. Earth Planet. Sci.* **31** 429–467.

Gadgil Sulochana and Gadgil Siddhartha 2006 The Indian monsoon, GDP and agriculture; *Economic and Political Weekly*, pp. 4887–4895.

Gadgil Sulochana, Joseph P V and Joshi N V 1984 Ocean–atmosphere coupling over monsoon regions; *Nature* **312** 141–143.

Gadgil Sulochana, Vinaychandran P N, Francis P A and Gadgil Siddhartha 2004 Extremes of Indian summer monsoon rainfall, ENSO, equatorial Indian Ocean Oscillation; *Geophys. Res. Lett.* **31**, https://doi.org/10.1029/2004GL019733.

Gadgil Sulochana, Francis P A, Vinayachandran P N and Sajani S 2020 Interannual variation of the Indian summer monsoon, ENSO, IOD and EQUINOO; In: *Monsoon Teleconnections* (eds) Jasti Chowdary, Anant Parekh and C Gnanaseelan, Elsevier Publications.

Graham Nicholas E and Barnett Tim P 1987 Sea surface temperature, surface wind divergence, and convection over tropical oceans; *Science* **238** 657–659.

Huang Boyin, Peter W Thorne, Viva F Banzon, Tim Boyer, Gennady Chepurin, Jay H Lawrimore, Matthew J Menne, Thomas M Smith, Russell S Vose and Huai-Min Zhang 2017 NOAA Extended Reconstructed Sea Surface Temperature (ERSST) Version 5; *NOAA National Centers for Environmental Information*, https://doi.org/10.7289/V5T72FNM.

Ihara Chie, Yochanan Kushnir, Mark A Cane and Victor H De La Pena 2007 Indian summer monsoon rainfall and its link with ENSO and Indian Ocean climate indices; *Int. J. Climatol.* **27** 179–187, https://doi.org/10.1002/joc.1394.

Izumo T, de Boyer Montégut C, Luo J J, Behera S K, Masson S and Yamagata T 2008 The role of the western Arabian Sea upwelling in Indian monsoon rainfall variability; *J. Climate* **21** 5603–5623.

Johnson N and Xie S P 2010 Changes in the sea surface temperature threshold for tropical convection; *Nature Geosci.* **3** 842–845.

Joseph P V 1976 *Proc. Symp. Tropical Monsoons*; Indian Institute of Tropical Meteorlogy Pune, 378p.

Kumar K, Rajagopalan Balaji, Hoerling Martin, Bates Gary and Cane Mark 2006 Unraveling the Mystery of Indian Monsoon Failure During El Nino; *Science* **314** 115–119, https://doi.org/10.1126/science.1131152.

Liebmann B and Smith C A 1996 Description of a complete (interpolated) outgoing longwave radiation dataset; *Bull. Am. Meteorol. Soc.* **77** 1275–1277.

Parthasarathy B A, Munot A and Kothawale D R 1994 All-India monthly and seasonal rainfall series: 1871–1993; *Theor. Appl. Climatol.* **49**(**4**) 217–224.

Rasmusson E M and Carpenter T H 1983 The relationship between the eastern Pacific sea surface temperature and rainfall over India and Sri Lanka; *Mon. Weather Rev.* **111** 354–384.

Reiter E R 1978 Long-term wind variability in the tropical Pacific, its possible causes and effects; *Mon. Weather Rev.* **106**(**3**) 324–330.

Saji N H, Goswami B N, Vinayachandran P N and Yamagata T 1999 A dipole mode in the tropical Indian Ocean; *Nature* **401** 360–363.

Sikka D R 1980 Some aspects of the large-scale fluctuations of summer monsoon rainfall over India in relation to fluctuations in the planetary and regional scale circulation parameters; *Proc. Indian Acad. Sci. (Earth & Planet. Sci.)* **89** 179–195.

Sun C, Li J, Kucharski F, Kang I S, Jin F F, Wang K *et al.* 2019 Recent acceleration of Arabian Sea warming induced by the Atlantic–western Pacific trans-basin multidecadal variability; *Geophys. Res. Lett.* **46** 1662–1671, https://doi.org/10.1029/2018GL081175.

Vecchi G A and Harrison D E 2004 Interannual Indian rainfall variability and Indian Ocean sea surface temperature

anomalies; *Geophys. Monogr. Ser., Am. Geophys. Union, Washington DC* **147** 3–9, https://doi.org/10.1029/147GM14.

Webster P J, Moore A M, Loschnigg J P and Leben R R 1999 Coupled ocean–atmosphere dynamics in the Indian Ocean during 1997–1998; *Nature* **401** 356–360.

Xie Shang-Ping, Deser Clara, Vecchi Gabriel, Ma Jian, Teng Haiyan and Wittenberg Andrew 2010 Global warming pattern formation: Sea surface temperature and rainfall; *J. Climate* **23**, https://doi.org/10.1175/2009JCLI3329.1.

Corresponding editor: Somnath Dasgupta